

Optimization of Microwave Packaging Structure for Directly Modulated Laser Modules Using Three-Dimensional Electromagnetic Model

Wei Han

Marc Rensing

Peter O'Brien

Integrated Photonics Group,
Tyndall National Institute,
Cork, Ireland

Frank H. Peters

Integrated Photonics Group,
Tyndall National Institute,
Cork, Ireland;
Department of Physics,
University College Cork,
Cork, Ireland

In this paper, the packaging aspects of directly modulated laser (DML) modules are investigated using detailed electromagnetic (EM) simulations. The packaging influences of the laser module are specified in two parts as RF connector and optoelectronic subsystem. By carefully optimizing the package structure, the simulation results show that the insertion loss of the proposed module is less than 1 dB up to 40 GHz. Then, a DML module is packaged and measured based on the optimized package scheme. A resonance free bandwidth of approximately 20 GHz is obtained with a 3 dB bandwidth of about 15 GHz. [DOI: 10.1115/1.4005292]

1 Introduction

As the advanced Fiber to the Subscriber and high-speed optical interconnections requires low cost and compact size transmitters. The semiconductor optical devices are playing an increasingly significant role to achieve high efficiency, wideband performance, and small factor packaging size. High-speed semiconductor laser diodes (LDs) are widely employed as the transmitters in Central Office (CO.) or customer terminals.

There have been many studies on the performance of high-speed LDs as well as the broadband laser modules [1–3]. Based on small signal equivalent circuit model, the transmission characteristics of the laser module can be investigated [2,3]. In Refs. [4] and [5], the package aspects of the laser chip as well as the optoelectronic devices are investigated. In this paper, a three-dimensional model of the directly modulated module (DML) with an RF connector is built using the commercially available simulator ANSOFT HFSS. With this model, the distributed package parameters of the laser module can be directly investigated and optimized. The insertion loss (IL) and the RF reflections in different parts of the module are evaluated, and the results show that the overall package has a transmission capability of 40 Gbps. The characteristics of higher-order resonances are also analyzed. The simulation results indicate that by carefully designing the RF

return path and the ground continuity, undesirable resonances can be efficiently suppressed. In Sec. 3, a DML module is packaged and measured to validate the proposed packaging structure.

2 EM Analysis of the DML Module

As a widely used packaging technology, the butterfly (BTF) package with RF connector exhibits excellent microwave characteristics and easily integrates with other components. Figure 1 shows a 3D electromagnetic (EM) model for the proposed BTF packaging scheme, which includes the BTF receptacle, the RF connector, and the optoelectronic subsystem. In this paper, the EM model is only defined for high-speed analysis, and the DC parts are not included to simplify the calculation. There are two key sections that need to be analyzed in detail. The first part is the RF connector and the feed-through. The second part is the optoelectronic subsystem consisting of the heat sink and the microwave transmission line.

Figure 2 shows the assembly of the RF connector. The RF connector is a commercially available V connector with a glass bead as the feed-through element. In Fig. 2, the RF path consists of coaxial transmission lines with different sizes of the center conductor. The impedance matching is realized by a corresponding change in the diameter of surrounding dielectric material. The multisection structure will bring discontinuities between the boundaries of the coaxial lines, which will induce extra reflections.

By tuning the ratio of D2 to D1, Fig. 3(a) shows the RF reflection (S_{11}) of the RF connector assembly. D1 and D2 are diameters of the center conductor in glass bead and RF connector,

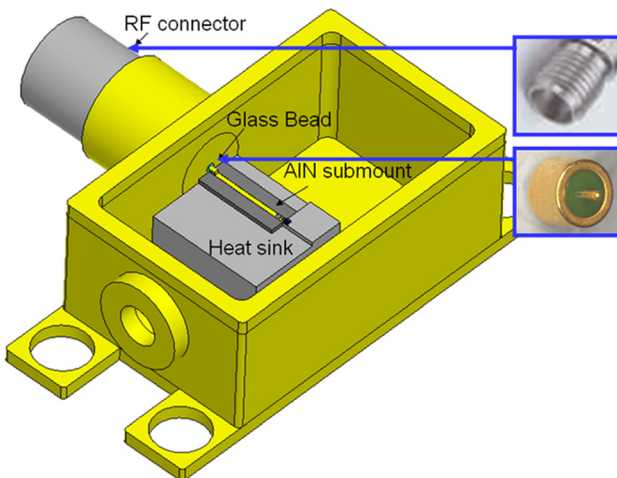


Fig. 1 EM model of the BTF package including the RF connector and glass bead

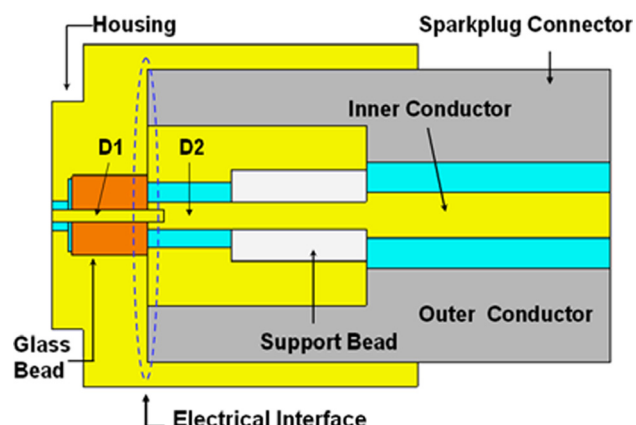


Fig. 2 Assembly of RF connector and glass bead

Contributed by the Electronic and Photonic Packaging Division of ASME for publication in the JOURNAL OF ELECTRONIC PACKAGING. Manuscript received October 11, 2010; final manuscript received August 31, 2011; published online December 9, 2011. Assoc. Editor: Stephen McKeown.

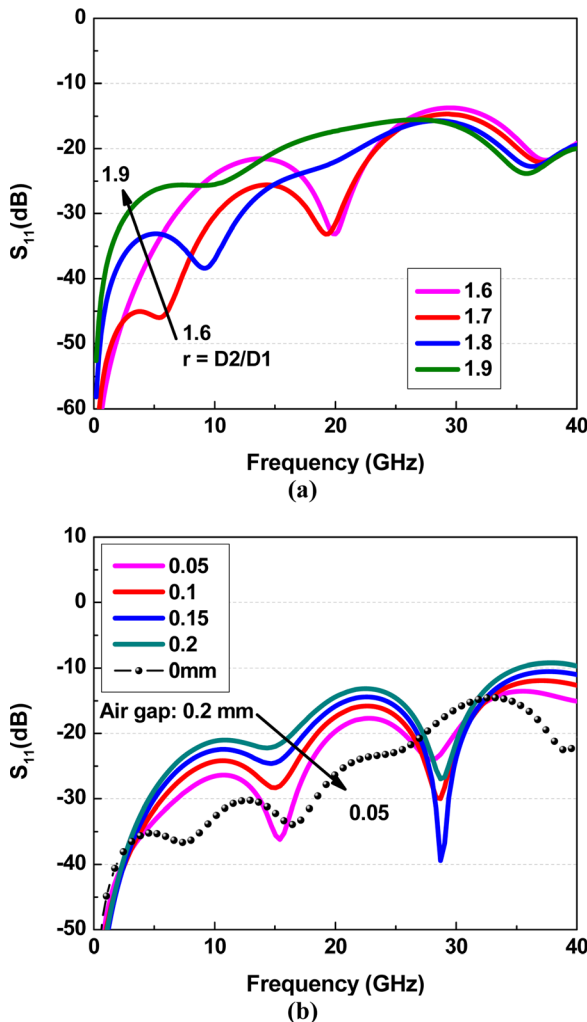


Fig. 3 Simulated reflection (S_{11}) with different (a) ratios of D_2/D_1 and (b) air gap values

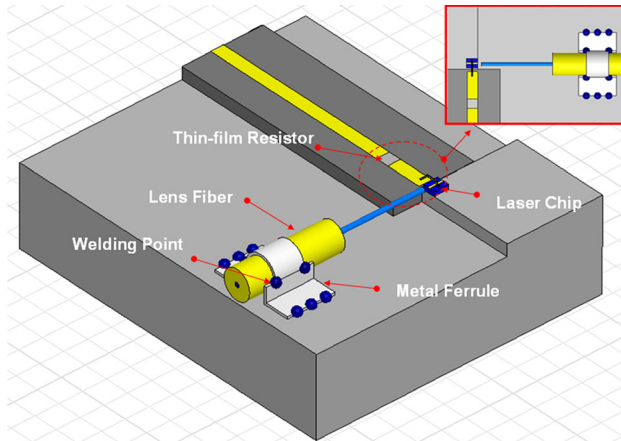


Fig. 4 Assembly structure for the optoelectronic subsystem

respectively. The results show a visible variety of S_{11} by adjusting the ratio from 1.6 to 1.9. An optimized value of 1.7 can provide a better performance especially below 25 GHz. Due to improper soldering or poor mechanical tolerance, an air gap may exist between the glass bead and RF connector, as the dashed line

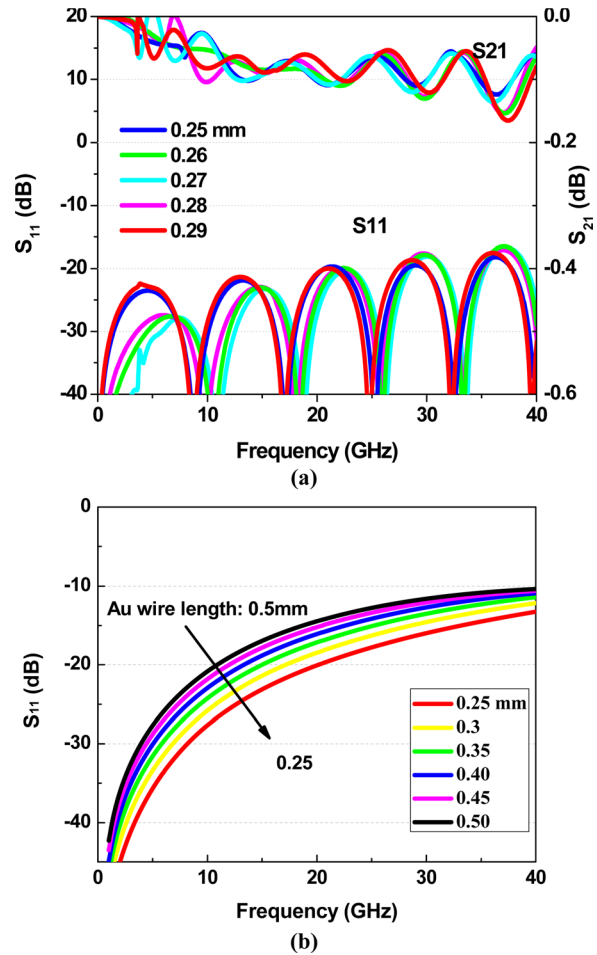


Fig. 5 (a) S_{21} and S_{11} of the MSL with different linewidths and (b) influence of the Au wire on reflection

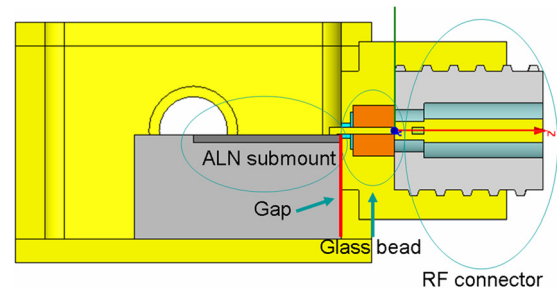


Fig. 6 Section plane of the RF signal transmission path

shown in Fig. 2. This air gap will bring extra RF reflection on the interface plane. Figure 3(b) shows the influence of such gap on RF reflection. It can be seen from the picture that with a gap value of 0.05 mm, the reflection S_{11} will increase from -35 dB to -27 dB at 10 GHz. When the gap is less than 0.15 mm, the assembly can provide a useful bandwidth up to 40 GHz with a reflection below -10 dB.

The optoelectronic subsystem assembly shown in Fig. 4 consists of a laser chip as well as the bonding wire, AlN ($Er = 8.7$) based microstrip line (MSL), Kovar heat sink, and the optic devices such as lens fiber and metal ferrule for laser welding. A 0.250 mm mesa is fabricated in the Kovar heatsink to shorten the Au bonding wire between the microstrip line and the laser chip. As a RF signal transmission path, the AlN submount should be

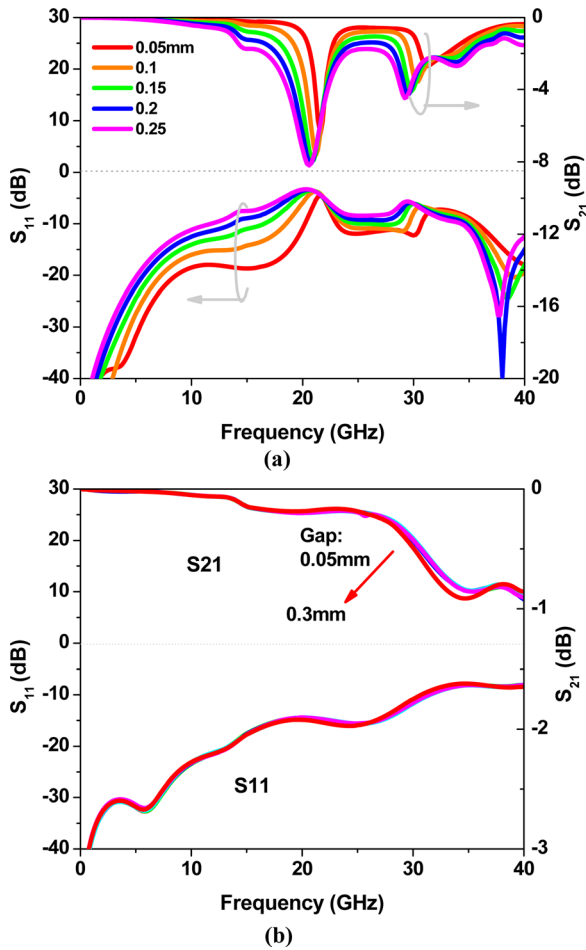


Fig. 7 (a) Resonances due to the improper optoelectronic subsystem assembly, and (b) results with optimization

designed carefully to have low insertion loss (S_{21}) and reflection (S_{11}). Figure 5(a) shows the optimization of this RF submount. The thickness of the ceramic submount is designed to 0.25 mm. The line width of the microstrip is finely tuned from 0.25 mm to 0.29 mm to optimize the broadband performance. In Fig. 5(a), the line width does not alter the S_{21} up to 40 GHz. However, an improved reflection performance at 10 GHz is obtained when the width is set at 270 μ m. the insertion loss and reflection of proposed RF submount at 40 GHz are approximately 0.14 dB and -18 dB, respectively.

In a general packaging scheme, the laser chip is connected to the RF submount by using an Au bonding wire. It will bring parasitic inductance and further degrade the reflection performances. Figure 5(b) shows the influence of the bonding wire by changing the wire length. When the Au wire increases from 0.25 mm to 0.5 mm, the reflection will be enhanced from -28 dB to -20 dB, which is in evidence that the RF performance will be greatly improved by shorten the length of the bonding wire.

Figure 6 shows the section plane of the RF signal transmission path. When mounting the optoelectronic subsystem into the BTF package, an effective ground connection should be formed between the optoelectronic subsystem and the sidewall of the BTF. If an air gap exists between these two parts, as shown in Fig. 6, a ground discontinuity will be introduced.

By enlarging the separation from 0.05 mm to 0.3 mm in 0.05 mm increment, the transmission performance is simulated. As shown in Fig. 7(a), resonance peaks are observed in the regions of 20 GHz and 30 GHz. A large notch is observed at approximately 20 GHz, and the magnitude of S_{21} undergoes a fast decay beyond 10 GHz. The bandwidth of the package is only 17 GHz when the

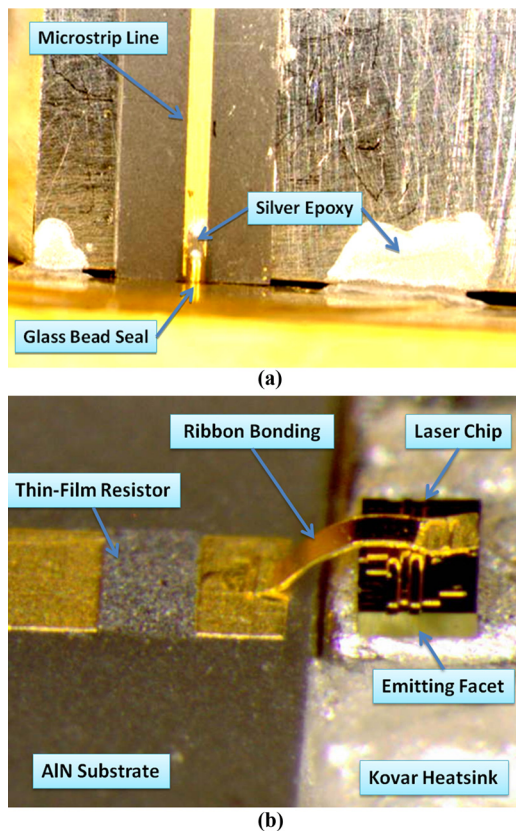


Fig. 8 Packaged laser module based on the optimized simulation results

gap is 0.3 mm. The cutoff bandwidth also exhibits an increased reflection of -10 dB at 10 GHz. This gap not only increases the RF return signal but also creates a discontinuity in the ground plane, and excites the high-order resonances. To validate our assumption, the package sidewall was connected to the Kovar heatsink similar to that shown in Fig. 8(a). It is evident from Fig. 7(b) that all resonances are efficiently suppressed by this improved ground contact. These results indicate that a stable and continuous ground contact is critical for high-speed optoelectronic packaging, especially in the transition region between different waveguides.

In Fig. 7(b), simulation results also show that the optimized overall package has an insertion loss of approximately 1 dB within the 40 GHz bandwidth, and the reflection is less than 10 dB up to 30 GHz. The above results indicate a resonance free performance and a transmission capability of 40 Gbps.

3 Fabrication and Test of the DML Module

Based on the optimized results from EM simulation, a DML module was packaged in our laboratory. Figures 8(a) and 8(b) show the package assembly details of the DML module. A 1.85 mm RF connector was employed with a Corning glass based glass bead, and the ratio of the contacting conductors is approximately 1.7 to provide better reflection performance. As the resistance of the laser chip used was approximately 5 Ω , a 45 Ω thin film NiCr resistor was integrated in the 270 μ m microstrip line to provide 50 Ω R matching. A 250 μ m Au ribbon bonding was used to connect the laser chip and the microstrip line. As shown in Fig. 8(a), the stable ground contact was enabled using silver epoxy.

Anritsu 37397D 65 GHz vector network analyzer (VNA) and Anritsu MN4765A 65 GHz detector module were used for the measurement. The laser module was biased at $I_{th}+25$ mA. As shown in Fig. 9(a), without signal path optimization, strong resonances and decay were observed. These intensive resonances

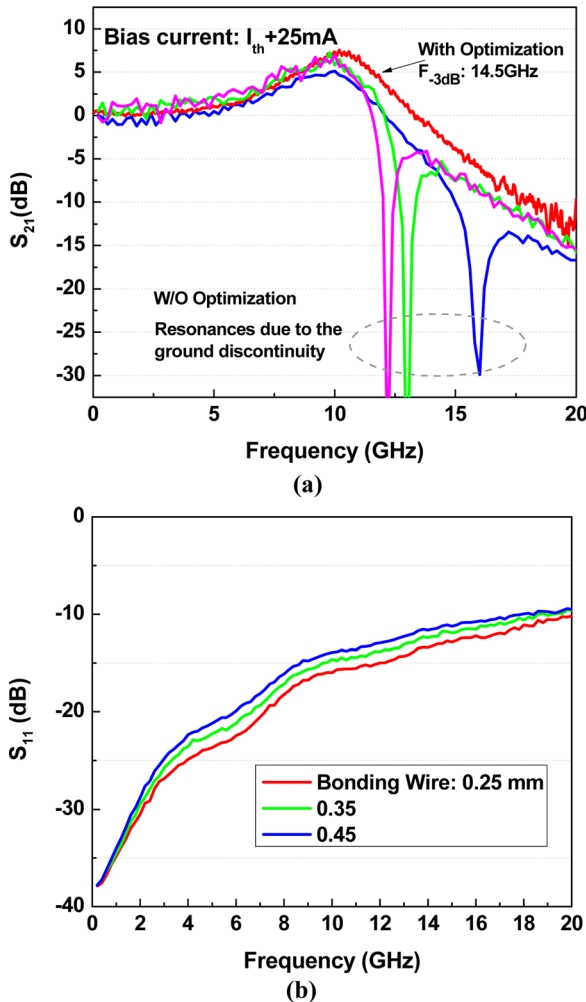


Fig. 9 (a) Measured S_{21} of DML module with and without optimization and (b) measured S_{11} with different Au wire lengths

may greatly affect the high-speed performance of the DML modules. By improving the ground continuity of proposed laser module, a resonance free 3 dB bandwidth of 14.5 GHz was achieved, and the frequency response was enhanced obviously beyond 10 GHz. Figure 9(b) shows the measured S_{11} to characterize the influence of the Au wire. It indicates that a 250 μm Au wire can provide a reflection of -16 dB at 10 GHz, which is improved by 1.5 dB and 2.5 dB compared with using 350 μm and 450 μm Au wire.

4 Conclusions

In this paper, the transmission characteristics of a DML package have been investigated using 3D EM simulation and experiment. Employing an RF connector and simple straight microstrip line, a transmission capability of 40 bps is obtained. Our results also indicate significant resonances arising from discontinuities in the ground plane. With improved ground contact, the influence of resonance on useful bandwidth was shown to be negligible. An optimized DML module was packaged and demonstrated a resonance free bandwidth up to 20 GHz.

Acknowledgment

This work was supported by SFI under Grant No. 07/SRC/I1173.

References

- [1] Han, W., Zhu, N. H., Xie, L., Ren, M., Sun, K., Zhang, B. H., Li, L., and Zhang, H. G., 2009, "Injection Locked Fabry-Perot Laser Diodes for WDM Passive Optical Network Spare Function," *Optics Communications*, **282**(17), pp. 3553–3557.
- [2] Zhang, S. J., Zhu, N. H., and Liu, Y., 2008, "Characterization of Parasitics From Scattering Parameters of Laser Diode," *Microwave Opt. Technol. Lett.*, **50**(1), pp. 1–4.
- [3] Chen, C., Zhu, N. H., and Zhang, S. J., 2007, "Characterization of Parasitics in TO-Packaged High-Speed Laser Modules," *IEEE Trans. Adv. Packag.*, **30**(1), pp. 97–103.
- [4] Alander, T. M., Heino, P. A., and Ristolainen, E. O., 2003, "Analysis of Substrates for Single Emitter Laser Diodes," *ASME J. Electron. Packag.*, **125**(3), pp. 313–318.
- [5] Ting, B., and Manno, V. P., 2005, "Transient Thermomechanical Simulation of Laser Hammering in Optoelectronic Package Manufacturing," *ASME J. Electron. Packag.*, **127**(3), pp. 299–305.